JETIR.ORG ISSN: 2349-5162 | ESTD Year : 2014 | Monthly Issue
JOURNAL OF EMERGING TECHNOLOGIES AND INNOVATIVE RESEARCH (JETIR)
An International Scholarly Open Access, Peer-reviewed, Refereed Journal

X-ray image based Covid-19 and Viral Pneumonia disease classification using Multiple Texture features and classification Methods

Suryakanth Baburao Ummapure[1], Ravindrakumar Tilekar[2]

[1]Government First Grade College, Shahapur, Karnataka, India.
[2]Government First Grade College, Bidar, Karnataka, India.

Abstract: *The covid-19 is a new disease emerged in Wuhan city from the People's Republic of China. This disease is mainly caused by a novel coronavirus known as SARS-Cov-2. To diagnose this disease doctors, consider the swab samples, Chest X-ray, and CT images of patients to detect the covid-19 disease. In order to identify the covid-19 disease, this study states classifying chest x-ray images. Three classes of chest x-ray images are used in the classification process. The first class is covid-19 affected, second, viral pneumonia, and last, normal x-ray image.LBP, HoG, and Gabor, three most widely used feature extraction techniques are taken into consideration to extract texture features from chest x-ray pictures. The standard dataset was used for an experiment. The dataset includes 3882 images. (1200 covid affected, 1341 viral pneumonia, and 1341 normal) x-ray images. To achieve the highest recognition accuracy, four popular classifiers (KNN, SVM, MLP, and RF) were engaged. The accuracy of recognition is reported in three categories (single, bi-features, and tri-features). HOG features using the MLP classifier and achieved the highest recognition accuracy of 96.30% in the individual features category. The Gabor with HOG features using MLP obtained 98.02% in the bi-features category, and the MLP classifiers' maximum recognition accuracy for tri-features was 98.19%. The novelty of this proposed paper the shrunken LBP features were used i.e., only 10 features* out of 59 features by changing the invariance of the input image to extract the features.

Keywords: ML, HOG, LBP, MLP, KNN,SVM, RF

1. INTRODUCTION

The advancement of computer vision systems benefits medical applications such as image enhancement, organ segmentation, and organ texture classification. The patient's chest X-ray images can reveal abnormalities of the patient. As a result of the disease, respiratory issues, heart damage, and secondary infection situations were observed. According to the findings, the COVID-19 virus spreads from person to person. The infected person requires treatment in an intensive care unit. Infected people have severe respiratory issues.

Classification of chest x-ray images to analyse the coronavirus affected images among viral pneumonia and normal person chest x-ray images. Hence, this paper has addressed the chest x-ray image classification based on texture features and multiple classification methods.

In the literature, some papers have been rapidly published during and virus pandemic. Many researchers are focused on this fascinating area and have given many challenging tasks regarding finding the virus-affected persons by observing the x-ray images. The fair analysis of the effect of the covid-19 virus has given in (Adnan et al., 2020), they have briefed the mainly two aspects; transmission and characteristics of this covid-19 coronavirus. The prediction of covid-19 by considering the X-ray images by using deep transfer learning is reported in (Minaee et al., 2020), and they have achieved the sensitivity of 97%(± 5%) by considering the pre-trained CNN models such as ResNet18,ResNet50, SqueezeNet, and DenseNet-121. The work reported in (Ozturk et al., 2020), has shown the automatic detection of Covid-19 cases by using DNN from X-ray images and they have obtained 98.00% classification accuracy. The clinical features of the corona virus-infected patients have given in (Huang et al., 2020) and they have reported the epidemiological, clinical, laboratory, and radiological characteristics and treatment and clinical outcomes of these patients. The classification of coronavirus based on CT images is given in (Özkaya et al., 2020), they have reported the classification accuracy of 96.09%. The novel deep neural network-based covid-19 detection by using the chest x-ray images have given in (Mangal et al., n.d.), and they have reported accuracy of 90.05%.

2. CHEST X-RAY DATASET

To carry out the experiment the standard publicly available database is used. Three kinds of images have taken for the experiments. First, covid-19 affected persons chest x-ray images from (https://github.com/armiro/COVID-CXNet) 1200 images, second virus pneumonia affected chest x-ray images from (https://www.kaggle.com/paultimothymooney/chest-xray-pneumonia) 1341 images and third is normal persons chest x-ray images from (https://www.kaggle.com/paultimothymooney/chest-xray-pneumonia) of 1341 the total of 3882 images have been used for the experiments. Following figure 1 shows the sample images

(i) Covid affected (ii) Viral pneumonia (iii) Normal

Figure 1. Sample Chest X-ray images

3. PROPOSED METHOD

This section contains the experiment part of the proposed work. The following figure 2. shows the block diagram of the proposed work.

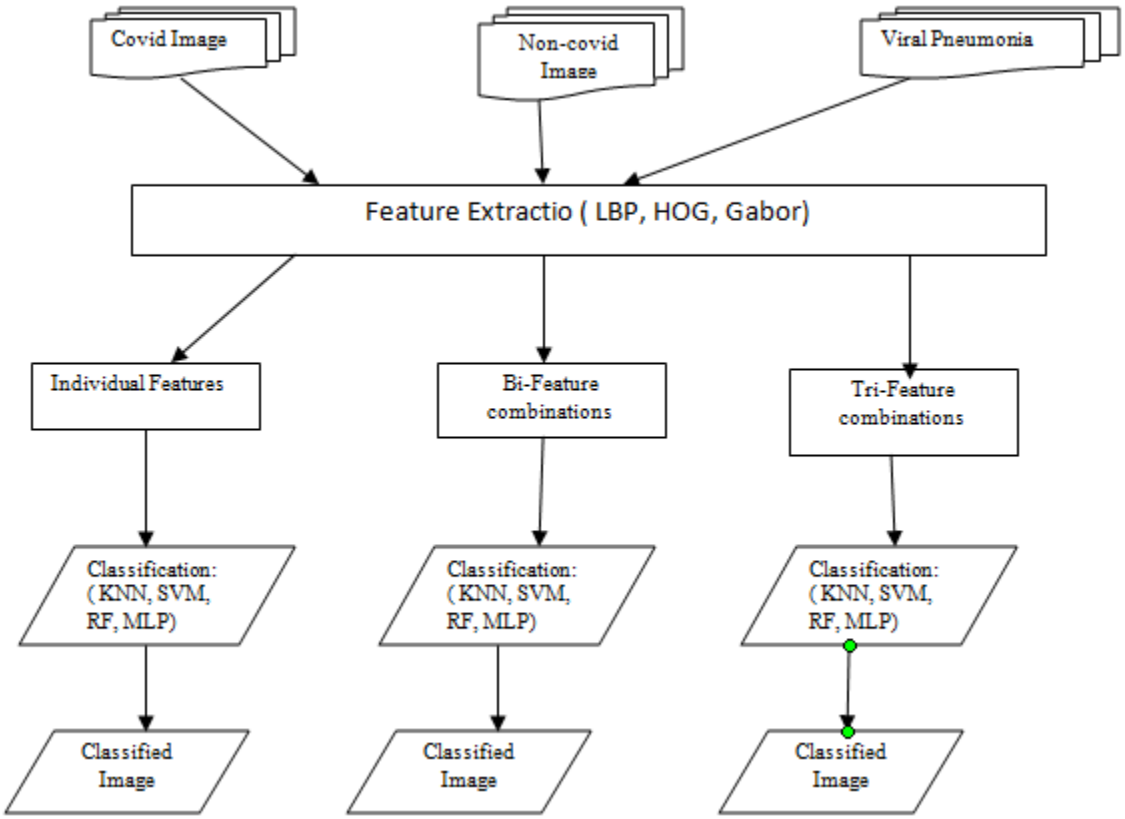

Figure 2. Block diagram of proposed method.

To extract the potential features the three kinds of feature extraction method were used. Those methods are LBP, Hog and Gabor, from these three methods the texture features are extracted. The details of feature extraction methods were given below.

1. **LBP (Local Binary Pattern):** This feature extraction method is widely used in face recognition and is now being used to extract prominent LBP features in many areas of research. (Camlica et al., 2016)(Tan & Triggs, 2007)(Liu et al., 2017)(PietikÃ¤inen, 2010)(Pietikäinen et al., 2011). The LBP feature is created by this way, first, it apply the sliding 3x3 mask over the image on each slide it thresholds the neighbouring pixels with center pixel. If the centre pixel is greater than or equal to neighbour pixel then in puts 1 and 0 otherwise. After all thresholding of full image, then it computes the histogram, then the histogram is normalize and by fixing upright option as false. The setting upright as false the LBP has give 10 dominant features. Following figure 3 shows the LBP computation.

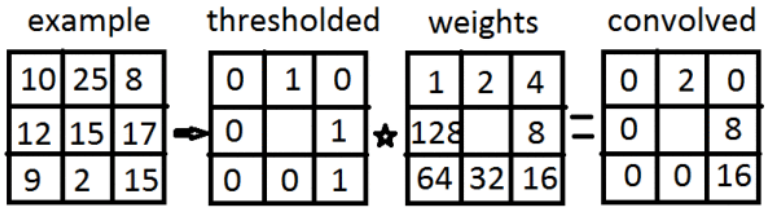

LBP = 2 + 8 + 16 = 26

C = (25+17+15)/3 - (10+8+12+9+2)/5 = -22

Figure 3. LBP computation

2. **HOG (Histogram oriented Gradients):** The HOG descriptor is concerned with an object's structure or shape (Jajoo et al., 2019)(Roy et al., 2012)(Mukhopadhyay et al., 2019)(P.S & V.S, 2016)(Mingqiang et al., 2008). It consideres edge features and HOG have the ability provide the direction edge also. Here the gradient and orientation or magnitude or orientation of the image edge is obtained. Like the LBP this HoG method also work in the sliding window fashion. But the difference is this HoG features taking the edge information of the image and whereas in LBP that thresholds pixel value on the sliding window. The following figure 4. Shows the input image after applying the HOG method .

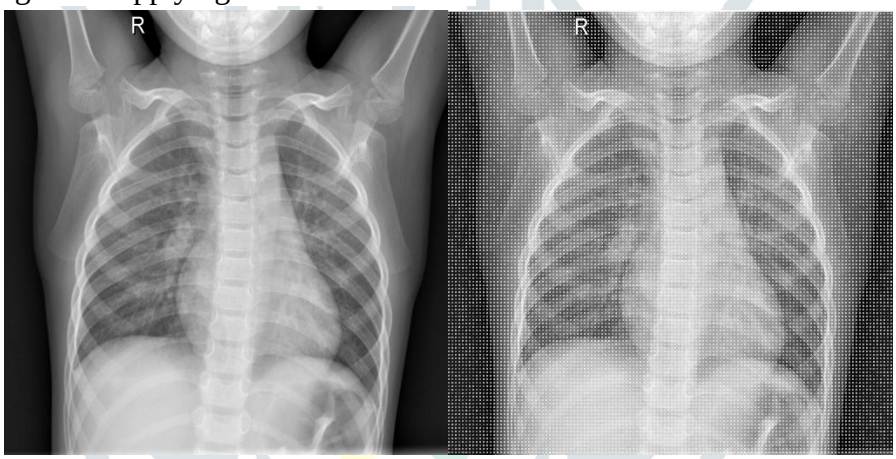

(i) Input Image (ii) Corrosponding HoG Image

Figure 4. Input image with corresponding HoG image.

3. **Gabor Features :** Gabor features are useful in extracting the features in the frequency domain. This method imitates the human visual perception, it projects the image in the angle and orientations this is called the bank of gabor filters. Usually, the mean energy and mean amplitude of each resulting output image are used as features.Assuming $g(x; y; \theta; \varphi)$ to be the function defining Gabor filter with θ being the spatial frequency and φ being the orientation,

we can define: $$g(x, y, \theta, \phi) = \exp(-\frac{x^2 + y^2}{\sigma^2}) \exp(2\pi\theta i(x \cos\phi + y \sin\phi)))$$

Where σ represents the standard deviation of the Gaussian kernel. In our study, we produce a bank of Gabor filters by considering 5 different scales and 6 orientations. The given text blocks are convolved with each of the filters and the mean energy and mean amplitude of the output images are used as features producing a 60 (30 × 2) dimensional feature vector(Malik et al., 2016).

To have the maximum recognition accuracy, the extracted features were made combinations in two and three feature combinations.

4. EXPERIMENTAL RESULTS AND DISCUSSION

This paper's primary goal is to classify x-ray images of covid, viral pneumonia, and normal patients. The three different types of images are fed into the proposed approach, which uses supervised classification algorithms to automatically classify the images based on the extracted features. KNN, SVM, MLP, and RF classifiers have all been used in this methodology to increase recognition accuracy. The following Tables shows the performance of the proposed methods. Below Table 1 shows the details of features, Table 2,3,4 shows the performance of the individual features.

Table 1. Details of Feature sets with average recognition accuracy

Sl. No.	Feature Set	Size of feature vector
1	LBP	10
2	HoG	81
3	Gabor	60
4	LBP,HoG	91
5	LBP,Gabor	70
6	Hog,Gabor	141
7	LBP,Hog,Gabor	151

Table 2. Average recognition accuracy for LBP features

Classification Results for LBP (10) Features							
Sl No.	Classifier	TP Rate	FP Rate	Precision	Recall	F-Measure	Rec. Acc
1	MLP	0.912	0.046	0.916	0.912	0.868	91.15%
2	KNN	0.862	0.071	0.865	0.862	0.862	86.18%
3	SVM	0.858	0.073	0.863	0.858	0.857	85.75%
4	RF	0.891	0.055	0.892	0.891	0.890	89.09%

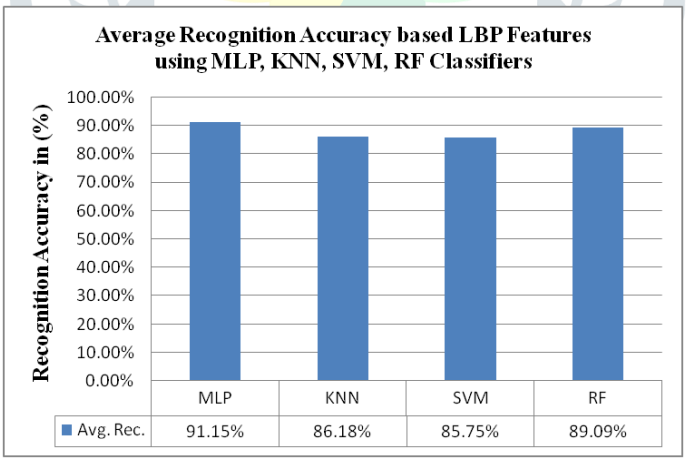

Figure 5. Performance of LBP features using MLP, KNN, SVM, and RF classifiers

Table 3. Average recognition accuracy for HoG features

Classification Results for HOG (81) Features							
Sl No.	Classifier	TP Rate	FP Rate	Precision	Recall	F-Measure	Rec. Acc
1	MLP	0.963	0.019	0.963	0.963	0.963	96.30%
2	KNN	0.930	0.036	0.931	0.93	0.930	92.96%
3	SVM	0.961	0.020	0.962	0.961	0.961	96.05%
4	RF	0.957	0.022	0.958	0.957	0.957	95.70%

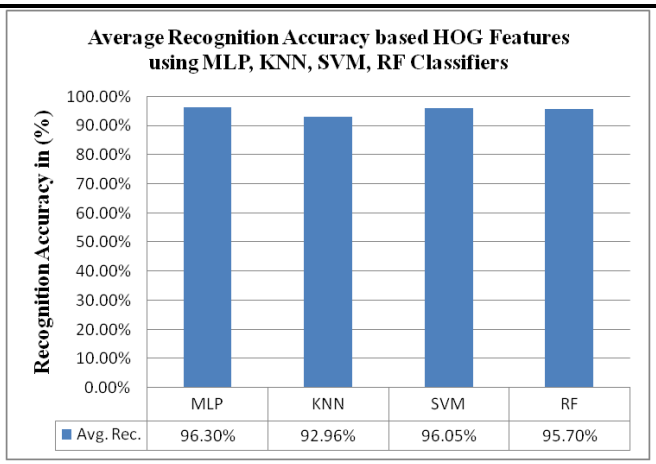

Figure 6. Performance of HoG features using MLP, KNN, SVM, and RF classifiers

Table 4. Average recognition accuracy for Gabor features

Classification Results for Gabor (60) Features							
Sl No.	Classifier	TP Rate	FP Rate	Precision	Recall	F-Measure	Rec. Acc
1	MLP	0.958	0.022	0.958	0.958	0.958	95.79%
2	KNN	0.931	0.035	0.934	0.931	0.932	93.13%
3	SVM	0.934	0.034	0.936	0.934	0.934	93.39%
4	RF	0.951	0.025	0.952	0.951	0.951	95.10%

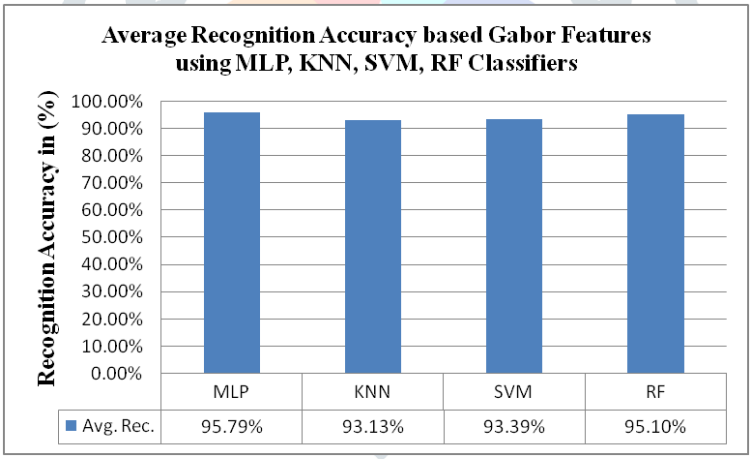

Figure 7. Performance of Gabor features using MLP, KNN, SVM, and RF classifiers

Following Table 5,6,7 shows the performance of the two feature combinations

Table 5. Average recognition accuracy for Gabor and LBP combined features

Classification Results for Gabor_LBP (70) Features							
Sl No.	Classifier	TP Rate	FP Rate	Precision	Recall	F-Measure	Rec. Acc
1	MLP	0.962	0.020	0.963	0.962	0.962	96.22%
2	KNN	0.941	0.031	0.942	0.941	0.941	94.07%
3	SVM	0.941	0.031	0.943	0.941	0.911	94.07%
4	RF	0.951	0.025	0.952	0.951	0.951	95.10%

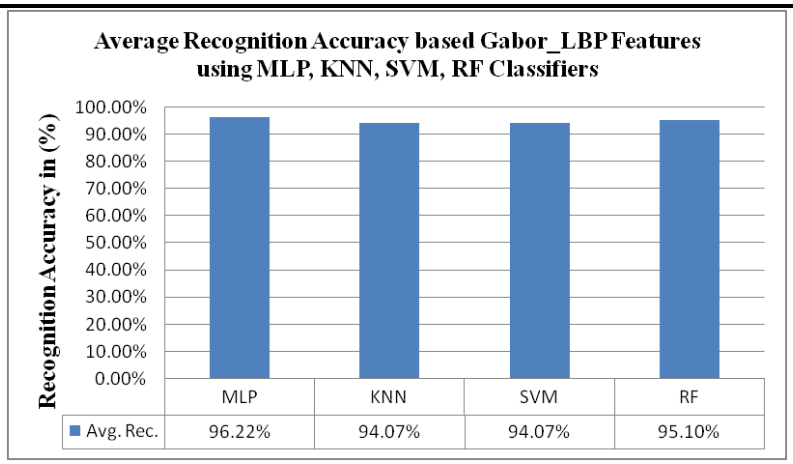

Figure 8. Performance of Gabor and LBP combined features by using MLP, KNN, SVM, and RF classifiers.

Table 6. Average recognition accuracy for HoG and LBP combined features

Classification Results for HOG _LBP (91) Features							
Sl No.	Classifier	TP Rate	FP Rate	Precision	Recall	F-Measure	Rec. Acc
1	MLP	0.964	0.019	0.964	0.964	0.946	96.39%
2	KNN	0.946	0.028	0.947	0.946	0.919	94.59%
3	SVM	0.956	0.022	0.957	0.956	0.956	95.62%
4	RF	0.961	0.020	0.962	0.961	0.961	96.13%

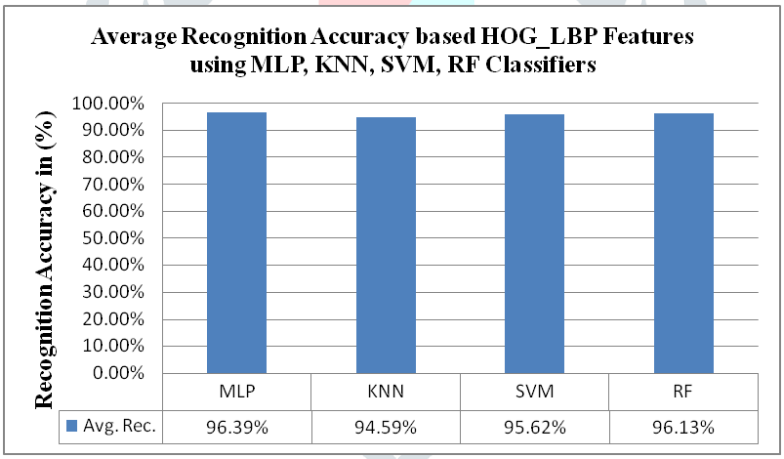

Figure 9. Performance of HoG and LBP combined features by using MLP, KNN, SVM, and RF classifiers.

Table 7. Average recognition accuracy for Gabor and HoG combined features

Classification Results for Gabor_HOG (141) Features							
Sl No.	Classifier	TP Rate	FP Rate	Precision	Recall	F-Measure	Rec. Acc
1	MLP	0.980	0.010	0.981	0.980	0.980	98.02%
2	KNN	0.945	0.028	0.946	0.945	0.945	94.50%
3	SVM	0.964	0.019	0.965	0.964	0.964	96.39%
4	RF	0.959	0.021	0.960	0.959	0.938	95.87%

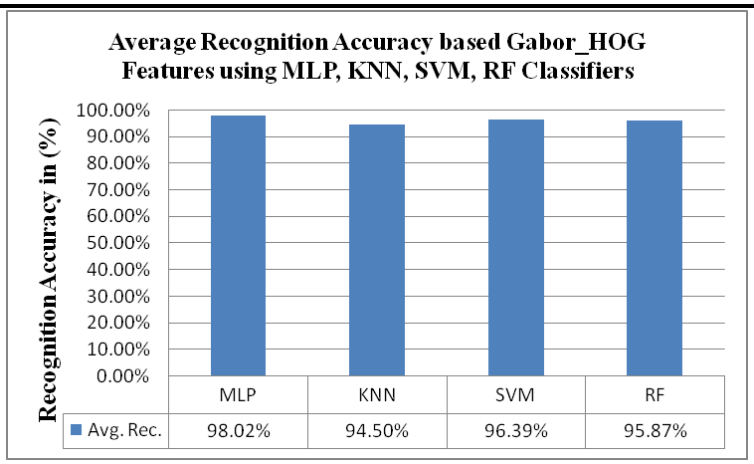

Figure 10. Performance of Gabor and HoG combined features by using MLP, KNN, SVM, and RF classifiers.

Following Table 8. Shows the performance of all three features combinations

Table 8. Average recognition accuracy for LBP, Gabor, and HoG combined features

Classification Results for Gabor_HOG _LBP (151) Features							
Sl No.	Classifier	TP Rate	FP Rate	Precision	Recall	F-Measure	Rec. Acc
1	MLP	0.912%	0.046	0.912	0.912	0.868	98.19%
2	KNN	0.862%	0.071	0.865	0.862	0.793	86.18%
3	SVM	0.858%	0.073	0.863	0.858	0.857	85.75%
4	RF	0.891%	0.055	0.892	0.891	0.89	89.09%

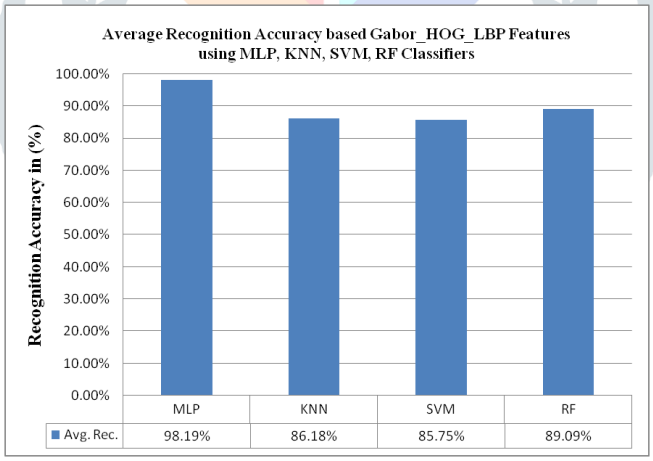

Figure 11. Performance of combination of LBP, HoG, and Gabor features by using MLP, KNN, SVM, and RF classifiers.

Following Table 9 and Table 10 exhibits the overall performance of an individual, two- features, and all feature combinations in the form of recognition accuracy.

Table 9. Average Recognition of Individual and Two-features combinations

Features	Classifiers	Avg. Rec. Acc.	Features	Classifiers	Avg. Rec. Acc.
LBP	MLP	91.15%	LBP, Hog	MLP	96.39%
	KNN	86.18%		KNN	94.59%
	SVM	85.75%		SVM	95.62%
	RF	89.09%		RF	96.13%
Hog	MLP	**96.30%**	LBP, Gabor	MLP	96.22%
	KNN	92.96%		KNN	94.07%
	SVM	96.05%		SVM	94.07%
	RF	95.70%		RF	95.10%
Gabor	MLP	95.79%	Gabor, HoG	MLP	**98.02%**
	KNN	93.13%		KNN	94.50%
	SVM	93.39%		SVM	96.39%
	RF	95.10%		RF	95.87%

Table 10. Average Recognition of Individual and Two-features combinations

Features	Classifiers	Avg. Rec. Acc.
LBP, Hog, Gabor	MLP	**98.19%**
	KNN	86.18%
	SVM	85.75%
	RF	89.09%

From the tables and figure it is noticed that in the individual features performance the HoG features are given highest recognition accuracy of 96.30%, in two-feature combinations Gabor with HoG features were given the maximum of 98.02% and at last all three features combinations the highest recognition is 98.19% from MLP classifier. Hence, it is described that the MLP has outperformed other classifiers viz., KNN, SVM, RF.

Following Table 11 shows the comparison analysis.

Table 11. Comparative analysis

Author	Method	Dataset_size	Features	Rec. Acc.
(Özkaya et al., 2020)	Shrunken Features	495	20	94.23%
Proposed	Combination of LBP,HoG and Gabor	3882	151	98.19%

The above comparison table shows the proposed method given good recognition accuracy with 3882 x-ray images with 151 features.

5. CONCLUSION

This paper presented the classification of the x-ray images in relation to covid-19 affected persons. The proposed method is given encouraging results as 98.19% is nearer to 100%. In this paper, the hand-crafted features were efficiently utilized due to the less no. of features and it not feasible to apply the deep learning architecture. Hence, in future work, the effort has been put to increase the dataset size and apply the deep learning methods.

Ethic of paper:

The findings are in this paper are restricted to experiment only and no human or animal trial has been taken for this experiment. This experiment is carried out on a publicly available standard dataset.

References

[1] Adnan, M., Khan, S., Kazmi, A., Bashir, N., & Siddique, R. (2020). COVID-19 infection : Emergence , transmission , and characteristics of human coronaviruses. *Journal of Advanced Research*, *24*, 91–98. https://doi.org/10.1016/j.jare.2020.03.005

[2] Camlica, Z., Tizhoosh, H. R., & Khalvati, F. (2016). Medical image classification via SVM using LBP features from saliency-based folded data. *Proceedings - 2015 IEEE 14th International Conference on Machine Learning and Applications, ICMLA 2015*, 128–132. https://doi.org/10.1109/ICMLA.2015.131

[3] Huang, C., Wang, Y., Li, X., Ren, L., Zhao, J., Hu, Y., Zhang, L., Fan, G., Xu, J., & Gu, X. (2020). *Articles Clinical features of patients infected with 2019 novel coronavirus in Wuhan , China*. 497–506. https://doi.org/10.1016/S0140-6736(20)30183-5

[4] Jajoo, M., Chakraborty, N., Mollah, A. F., Basu, S., & Sarkar, R. (2019). Script Identification from Camera-Captured Multi-script Scene Text Components. In *Advances in Intelligent Systems and Computing* (Vol. 740). Springer Singapore. https://doi.org/10.1007/978-981-13-1280-9_16

[5] Liu, P., Guo, J. M., Chamnongthai, K., & Prasetyo, H. (2017). Fusion of color histogram and LBP-based features for texture image retrieval and classification. *Information Sciences*, *390*, 95–111. https://doi.org/10.1016/j.ins.2017.01.025

[6] Malik, Z., Mirza, A., Bennour, A., Siddiqi, I., & Djeddi, C. (2016). Video Script Identification Using a Combination of Textural Features. *Proceedings - 11th International Conference on Signal-Image Technology and Internet-Based Systems, SITIS 2015, November*, 61–67. https://doi.org/10.1109/SITIS.2015.15

[7] Mangal, A., Kalia, S., Rajagopal, H., & Rangarajan, K. (n.d.). *CovidAID : COVID-19 Detection Using Chest*. 1–10.

[8] Minaee, S., Kafieh, R., Sonka, M., Yazdani, S., & Soufi, G. J. (2020). *Deep-COVID : Predicting COVID-19 From Chest X-Ray Images Using Deep Transfer Learning*. *April*.

[9] Mingqiang, Y., Kidiyo, K., & Joseph, R. (2008). A Survey of Shape Feature Extraction Techniques. *Pattern Recognition Techniques, Technology and Applications*. https://doi.org/10.5772/6237

[10] Mukhopadhyay, A., Kumar, S., Chowdhury, S. R., Chakraborty, N., Mollah, A. F., Basu, S., & Sarkar, R. (2019). Multi-Lingual Scene Text Detection Using One-Class Classifier. *International Journal of Computer Vision and Image Processing*, *9*(2), 48–65. https://doi.org/10.4018/ijcvip.2019040104

[11] No Title. (n.d.). https://www.covid19india.org/

[12] No Title. (2021). https://www.worldometers.info/coronavirus/#countries

[13] Özkaya, U., Öztürk, Ş., Budak, S., Melgani, F., & Polat, K. (2020). *Classification of COVID-19 in Chest CT Images using Convolutional Support Vector Machines*. *19*(December 2019), 1–20.

[14] Ozturk, T., Talo, M., Azra, E., Baran, U., & Yildirim, O. (2020). *Since January 2020 Elsevier has created a COVID-19 resource centre with free information in English and Mandarin on the novel coronavirus COVID-19 . The COVID-19 resource centre is hosted on Elsevier Connect , the company ' s public news and information . January*.

[15] P.S, S. K., & V.S, D. (2016). Extraction of Texture Features using GLCM and Shape Features using Connected Regions. *International Journal of Engineering and Technology*, *8*(6), 2926–2930. https://doi.org/10.21817/ijet/2016/v8i6/160806254

[16] PietikÃ¤inen, M. (2010). Local Binary Patterns. *Scholarpedia*, *5*(3), 9775. https://doi.org/10.4249/scholarpedia.9775

[17] Pietikäinen, M., Hadid, A., Zhao, G., & Ahonen, T. (2011). *Computer Vision Using Local Binary Patterns* (Vol. 40). https://doi.org/10.1007/978-0-85729-748-8

[18] Roy, K., Subrahmanya, G., & Rao, V. (2012). Combining feature descriptors for efficient classification and recognition of images. *2012 5th International Congress on Image and Signal Processing, CISP 2012*, *Cisp*, 420–424. https://doi.org/10.1109/CISP.2012.6470022

[19] Tan, X., & Triggs, B. (2007). Fusing gabor and LBP feature sets for kernel-based face recognition. *Lecture Notes in Computer Science (Including Subseries Lecture Notes in Artificial Intelligence and Lecture Notes in Bioinformatics)*, *4778 LNCS*, 235–249. https://doi.org/10.1007/978-3-540-75690-3_18

[20] G. G. Rajput and S. B. Ummapure, "Script Identification from Handwritten document Images Using LBP Technique at Block level," *2019 International Conference on Data Science and Communication (IconDSC)*, Bangalore, India, 2019, pp. 1-6, doi: 10.1109/IconDSC.2019.8816944

[21] Suryakanth Baburao Ummapure "Script Identification from Handwritten Document Images Using LBP features "International Journal of Computational Engineering Research (IJCER), vol. 08, no. 09, 2018, pp 13-21s